Biophysical Journal Volume 71 December 1996 3136–3147

Block of the cGMP-Gated Cation Channel of Catfish Rod and Cone Photoreceptors by Organic Cations

Stephanie C. Stotz and Lawrence W. Haynes
Department of Physiology and Biophysics, and Neuroscience Research Group, Faculty of Medicine, University of Calgary, Calgary, Alberta T2N 4N1, Canada

ABSTRACT Tetraalkylammonium compounds and other organic cations were used to probe the structure of the internal and external mouths of the pore of cGMP-gated cation channels from rod and cone photoreceptors. Both rod and cone channels were blocked by tetramethyl- through tetrapentylammonium from the intracellular side in a voltage-dependent fashion at millimolar to micromolar concentrations. The dissociation constant at 0 mV ($K_{D(0)}$) decreased monotonically with increasing carbon chain length from ~80 mM (TMA) to ~80 μM (TPeA), where the dissociation constant in rod channels is ~50% that of cone channels. *N*-Methyl-D-glucamine and the buffer Tris also blocked the cone channel in a voltage-dependent fashion at millimolar concentrations, but with lower affinity than similarly sized tetraalkylammonium blockers. Block by tetrahexylammonium (THxA) was voltage-independent, suggesting that the diameter of the intracellular mouth of these channels is less than the size of THxA but larger than TPeA. The location of the binding site for intracellular blockers was ~40% across the voltage-drop from the intracellular side. The addition of one carbon to each of the alkyl side chains increased the binding energy by ~4 kJ mol^{-1}, consistent with hydrophobic interactions between the blocker and the pore. Cone, but not rod, channels were blocked by millimolar concentrations of extracellular TMA. The location of the extracellular binding site was ~13% of the voltage drop from the extracellular side. In cone channels, the two blocker binding sites flank the location of the cation binding site proposed previously.

INTRODUCTION

The cGMP-gated ion channels of rod and cone photoreceptor outer segments are the last elements in the phototransduction cascade (reviewed in Stryer, 1986; Lagnado and Baylor, 1992). When these channels close in response to illumination, the decrease in current into the outer segment hyperpolarizes the cell and creates the electrical response to light. The channels of both rod (Furman and Tanaka, 1990; Menini, 1990; Colamartino et al., 1991; Zimmerman and Baylor, 1992) and cone (Picones and Korenbrot, 1992; Haynes, 1995a,b) are nonspecific cation channels that are partially blocked by divalent cations (Yau and Haynes, 1986). In the absence of divalent cations, the conductance of the rod channel is 25 pS (Haynes et al., 1986; Zimmerman and Baylor, 1986; Taylor and Baylor, 1995), whereas that of the cone channel is 50 pS (Haynes and Yau, 1990; Haynes, 1995a). In the presence of physiological concentrations of divalent cations, the conductance of the rod channel is reduced to 0.1 pS (Bodoia and Detwiler, 1985; Gray and Attwell, 1985), whereas the conductance of the cone channel is 2 pS (Haynes, 1995b). This difference between rod and cone channels is due in part to the higher conductance of divalent cations through the cone channel (Perry and McNaughton, 1991; Haynes, 1995b). These findings suggest that the structure of the permeation pathway in rods and cones should be different.

Using the tools of molecular biology, it has been shown that the rod (Kaupp et al., 1989), cone (Bönigk et al., 1993) and olfactory (Dhallan et al., 1990; Ludwig et al., 1990) cyclic nucleotide gated channels are structurally related to potassium channels (Jan and Jan, 1990). Like potassium channels, tetraalkylammonium compounds cannot pass through the cGMP-gated channels of rods (Picco and Menini, 1993) and cones (Picones and Korenbrot, 1992). We have used tetraalkylammonium compounds, together with Tris and *N*-methyl-D-glucamine, as probes of the physical and electrical structure of the internal and external mouths of the pore of rod and cone cGMP-gated cation channels to establish the position and physical characteristics of the blocker binding site. Our findings are consistent with the overall similarity of cyclic nucleotide-gated channels and potassium channels, and confirm the location of the permeant ion-binding site in cone channels inferred from Eyring rate theory models of ion permeation (Haynes, 1995b).

Some of these results have been briefly described in abstract form (Haynes, 1993; Stotz and Haynes, 1995).

METHODS

The preparation has been extensively described elsewhere (e.g., Haynes and Yau, 1990; Haynes, 1995a,b). Briefly, inside-out patches of plasma membrane were excised from the sides of catfish (*Ictalurus punctatus*) rod outer segments or the tips of cone outer segments and held under voltage clamp. Pipettes were pulled from thick-walled Corning 7740 borosilicate glass capillaries (A-M Systems, Everett, WA), coated with Sylgard 184 (Dow Corning Co., Midland, MI), and fire polished. In some experiments, the pipette was perfused by threading a thin quartz canula to within 1 mm of the electrode tip. The perfusate was controlled using a pressure regula

Received for publication 21 June 1996 and in final form 27 August 1996.

Address reprint requests to Dr. L.W. Haynes, Department of Physiology and Biophysics, University of Calgary, 3330 Hospital Dr. NW, Calgary, Alberta T2N 4N1, Canada. Tel.: 403-220-5011; Fax: 403-283-8731; E-mail: haynes@acs.ucalgary.ca.

© 1996 by the Biophysical Society

0006-3495/96/12/3136/12 $2.00

tion system (2PK+; Adams and List Associates, Westbury, NY), consisting of a pressure regulator, a perfusion bomb (or vial) containing the perfusate, and polyethylene tubing connecting the bomb to the quartz canula. The flow of perfusate was started by pressurizing the bomb.

The basic solution used in all experiments was buffered saline consisting of (in mM) 120 NaCl, 0.1 NaEGTA, 0.1 NaEDTA, and 5.0 NaHEPES (pH 7.6). Compounds used to block the channel were substituted for sodium on an equimolar basis. The following compounds were used: tetramethylammonium (TMA), tetraethylammonium (TEA), tetrapropylammonium (TPrA), tetrabutylammonium (TBA), tetrapentylammonium (TPeA), tetrahexylammonium (THxA), 2-amino-2-hydroxymethyl-1,3-propanediol (Tris), *N*-methyl-D-glucamine (NMDG), and choline. All tetraalkylammonium compounds were obtained from Aldrich (St. Louis, MO); choline, Tris, and NMDG were obtained from Sigma (St. Louis, MO). The concentrations of these compounds are given in the text. In some experiments the concentration of sodium was reduced while tonicity was maintained by the admixture of sucrose. In all experiments, channels were maximally activated by the addition of 1 mM cGMP (sodium salt, Sigma) to the bath solution.

Current-voltage relations were obtained using pairs of voltage ramps over a range of ±80 mV (Haynes, 1995a). From the initial holding potential of 0 mV, the first ramp was run from −80 mV to +80 mV, and the second was run from +80 mV to −80 mV. Both ramps were run at 120 mV s^{-1}. The resulting capacitive currents were removed by averaging the currents obtained at each voltage for the pair of ramps. Currents obtained before and after cGMP exposure were averaged together and subtracted from the currents in the presence of cGMP to obtain the net cGMP-dependent current. All currents presented here were leak subtracted in this way. Electrical signals were filtered with a DC−2.8 kHz bandwidth and digitized to the computer hard disk at 1 kHz. Although this violates the Nyquist rule, the actual current waveform (a 1.3-s ramp) is slow relative to the digitization rate, and so aliasing was not a problem. The use of ramps in blocking experiments can be problematic unless the duration of block is much less than the ramp duration. Given the modest increases in noise in the presence of blocker (Figs. 1–4, 7–9) and dissociation constants in the millimolar range, these appear to be fast blockers, and so the use of ramps is reasonable.

Data were analyzed by measuring the currents at 10-mV increments from plots of the current-voltage relations. Because of the reduction of sodium concentration in some experiments (notably TMA, NMDG, and Tris), a shift in reversal potential occurred. Currents were therefore converted to conductances for further analysis to account for the change in driving force, and the conductances were corrected for the lower ion activity using the concentration dependence of conductance described by Haynes (1995a). The fractional block of the conductance in the presence of a blocker was calculated as

$$FB = (g_{Max} - g_B)/g_{Max}, \quad (1)$$

where FB is the fraction of the conductance blocked, g_B is the conductance in the presence of blocker, and the conductance in the absence of blocker is g_{Max}. Plots of the fractional block as a function of concentration were fitted with either the Michaelis or Hill equations. Plots of fractional block as a function of voltage were fitted with the Woodhull equation (Woodhull, 1973):

$$FB = \frac{1}{1 + \frac{K_{D(0)}\exp(-z\delta FV/RT)}{[B]}}, \quad (2)$$

where $K_{D(0)}$ is the dissociation constant at 0 mV, [B] is the concentration of the blocker, V is the membrane potential, δ is the fraction of the voltage drop crossed by the blocker to reach its binding site, z is the valence of the blocker (+1 in all cases here), and F, R, and T have their usual thermodynamic meanings. The energy of interaction between the blocker and the channel can be calculated from

$$\Delta G = RT\ln(K_{D(0)}), \quad (3)$$

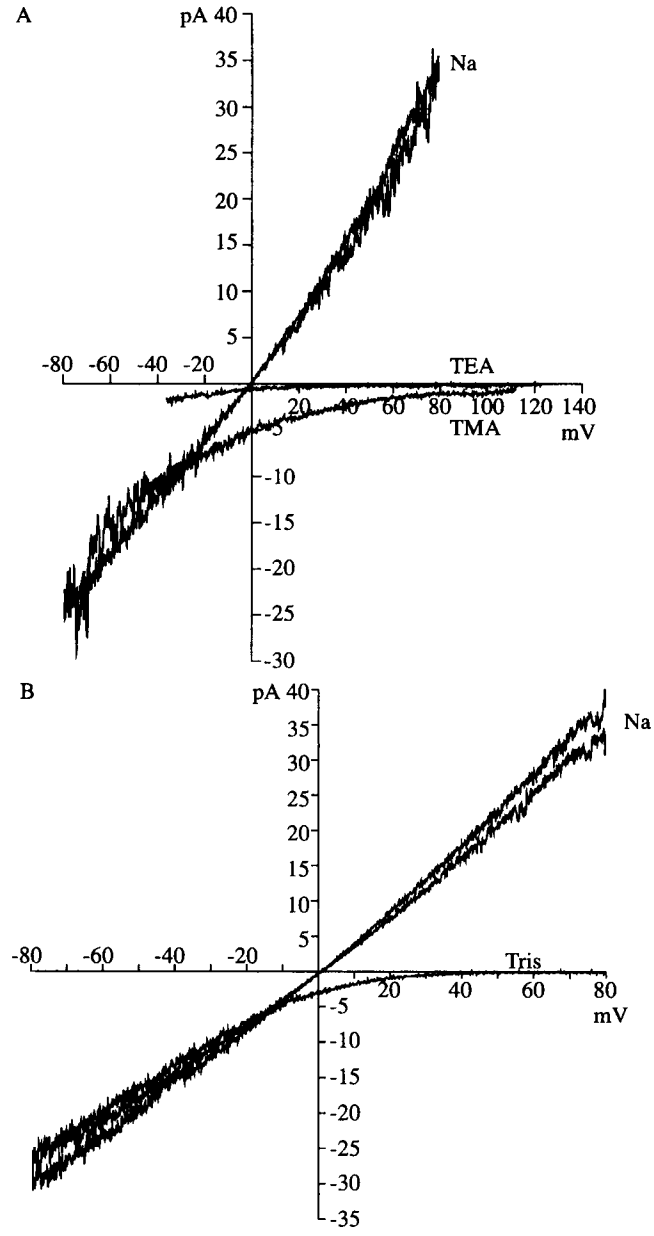

FIGURE 1 Substituted ammonium compounds are impermeant in cone channels. The indicated organic cation (120 mM) was present on the cytoplasmic side of the patch, and sodium (120 mM) was present on the extracellular side. (*A*) TMA and TEA did not support outward current under biionic conditions and partially blocked inward sodium current. Two traces for sodium are shown, one obtained before and one after the TMA and TEA trials. (*B*) Tris did not support outward current but produced little or no block of inward current. The two traces with Na were obtained before and after the Tris trials. Different patch from that in *A*.

where ΔG is the free energy of interaction.

In experiments where the pipette was perfused, the concentration of the blocker in the perfusate was diluted by the solution in the pipette. The concentration of sodium in the pipette could be calculated from the reversal potential using the Nernst equation. Using a sodium-sensitive electrode and a series of TMA/Na mixtures, a calibration curve was constructed relating the Nernst potential to the sodium and TMA concentrations. Once the sodium activity had been estimated, the concentration of TMA bathing the extracellular surface of the patch could then be calculated using this calibration curve.

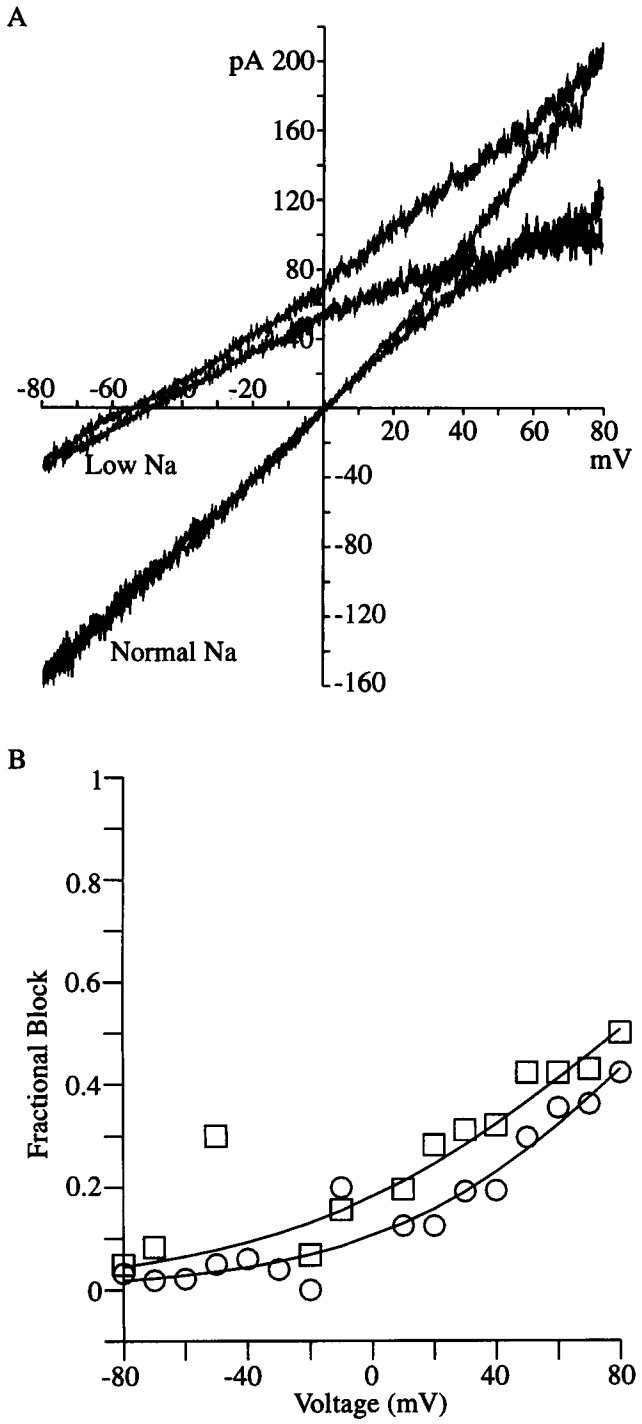

FIGURE 2 Block of the cone channel by internal TBA is affected by external ions. External sodium was reduced by perfusing the pipette with 10 mM sodium and 220 mM sucrose. (*A*) Current-voltage relations. The effects of 0.2 mM TBA on cone cGMP-dependent currents were assessed in normal and reduced sodium. Under both conditions, TBA blocked current in a voltage-dependent fashion. Replacement of extracellular sodium with sucrose caused a −50-mV shift in the reversal potential, as predicted by the Nernst equation. Traces through the origin are those obtained in normal sodium. (*B*) Voltage dependence of block. The fraction of conductance blocked by 0.2 mM TBA in the normal and low extracellular sodium is shown as a function of voltage. Solid lines are fits of Eq. 2 to the data. In normal extracellular sodium (F), $K_{D(0)}$ was 1.70 mM and δ was 0.599. In the presence of decreased external sodium (G), $K_{D(0)}$ was 0.903 mM and δ was 0.495.

Throughout, data are presented as mean ± standard deviation. Statistical tests were two-sided, one- or two-sample Student's *t*-tests, unless otherwise indicated. Tests for regression slopes and intercepts were obtained from Zar (1984).

RESULTS

Permeability of organic monovalent cations

The Woodhull equation (Eq. 2) makes two assumptions about the nature of the blocker that must be true if the values obtained for the dissociation constant at 0 mV ($K_{D(0)}$) and the electrical distance crossed to the binding site (δ) are to be meaningfully interpreted. First, the blocker must be impermeant. If the blocker is permeant then the value for δ will be underestimated. The permeability of ions can be tested by measuring the reversal potentials under biionic conditions (i.e., with only sodium in the pipette and only organic cation in the bath). Under these conditions, ammonium easily permeates the cGMP-gated channels of both rods (Furman and Tanaka, 1990; Picco and Menini, 1993) and cones (Haynes, 1995a), with both permeability and conductance greater than that of sodium. However, it is clear that the substituted ammonium compounds TMA and TEA are impermeant in cone channels (Fig. 1 *A*), because none of these ions supported outward current (n = 14 for TMA, 11 for TEA). In addition, TMA and TEA at least partially blocked the inward flux of sodium, and the degree of block increased with increasing length of the substituting carbon chain. This suggests a role for hydrophobic interactions in the block, as has been found for potassium channels (see Yellen, 1987, for a review). TPrA, choline, and NMDG (n = 2 for each) showed behavior similar to that of TMA and TEA under biionic conditions (data not shown). These findings are similar to those in the rod channel (Menini, 1990; Picco and Menini, 1993) and agree with the observation of Picones and Korenbrot (1992) that TMA is impermeant in bass cones. The widely used buffer Tris was also impermeant (Fig. 1 *B*, n = 4), but unlike the tetraalkylammonium compounds did not appear to block the inward current. However, it did block outward current when mixed with sodium on the cytoplasmic side of the channel (see below).

Tetraalkylammonium compounds occlude the pore

The second assumption of the Woodhull equation is that the blocker acts by entering the pore and crossing a portion of the transmembrane voltage drop before reaching its binding site, resulting in voltage-dependent block. However, interactions of the blocker with a voltage-sensitive process such as gating could also produce voltage-dependent "block." The voltage dependence of the gating process in rods is quite weak (Karpen et al., 1988a,b; Taylor and Baylor, 1995), and the open probability of the fully liganded cone channel is voltage independent (Haynes, 1995a). However,

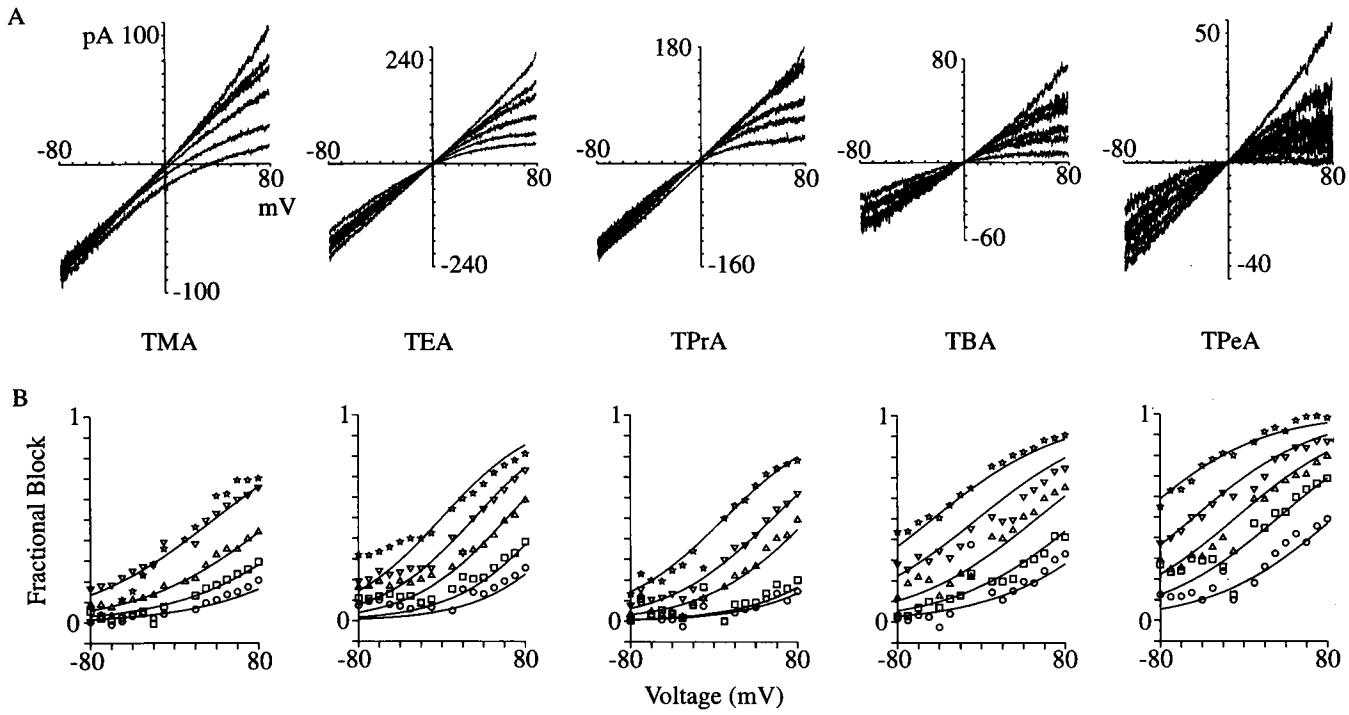

FIGURE 3 Tetraalkylammonium compounds block the cone channel from the cytoplasmic side. TMA, TEA, TPrA, TBA, or TPeA (from left to right) was substituted on an equimolar basis for sodium on the cytoplasmic side of the channel. (*A*) Current-voltage relations. Each plot represents data obtained from a different patch. In these experiments, TMA was applied in concentrations of 0, 5, 10, 20, 50, and 100 mM; TEA, 0, 1, 2, 5, 10, and 20 mM; TPrA, 0, 0.2, 0.25, 1, 2, and 5 mM; TBA, 0, 0.05, 0.1, 0.2, 0.5, and 1 mM; TPeA, 0, 0.02, 0.05, 0.1, 0.2, and 0.5 mM. The shift in reversal potential observed for TMA can be accounted for by the change in the Nernst potential for sodium. (*B*) Fractional block as a function of voltage for each of the current-voltage relations in *A*. Symbols represent the different concentrations of blocker (○, □, △, ▽, and ☆, from lowest to highest). Solid lines are fits of Eq. 2, with all points in a given plot fitted simultaneously. Data obtained in the presence of 100 mM TMA were considered unreliable because of a change in patch seal resistance and were not included in the fits. $K_{D(0)}$ and δ for each patch were (respectively) 91 mM and 0.40 for TMA, 7 mM and 0.37 for TEA, 6.5 mM and 0.50 for TPrA, 0.47 mM and 0.41 for TBA, and 0.089 mM and 0.43 for TPeA.

individual conformational changes that occur during the cone gating process may have voltage-sensitive components (Haynes, 1992; Haynes and Stotz, 1996). If the blockers we are using interfere with some voltage-sensitive stage of the gating process, then describing the resulting decrease in conductance by the Woodhull model is inappropriate and the values obtained are meaningless. If, on the other hand, the blocker occupies a site within the pore, then the probability that the blocker rather than a permeant ion occupies the channel should be reduced by permeant ions entering the channel from the opposite side. This competition would be reduced if the concentration of permeant ions in the extracellular solution were reduced, and under these conditions a decrease in $K_{D(0)}$ should be observed. Such a decrease would not be expected if, for example, the blocker acted at some allosteric site on the cytoplasmic side of the channel.

The concentration of sodium on the extracellular side of the cone channel was reduced by perfusing the pipette with a 10 mM sodium solution. In the absence of an inert substituting ion for sodium, sucrose was used to maintain the tonicity of the pipette solution. Tetrabutylammonium (TBA) applied to the intracellular side of the patch blocked the current in both normal and low extracellular sodium (Fig. 2 *A*). However, the fractional block of conductance by TBA as a function of voltage (Fig. 2 *B*) in low extracellular sodium was greater than in high extracellular sodium, indicating a decrease in $K_{D(0)}$. In three experiments, $K_{D(0)}$ as estimated by fitting Eq. 2 was reduced by 68 ± 18% in the presence of low extracellular sodium. Because sucrose is uncharged, the surface potential should become more negative as the ionic strength is reduced. Based on the estimated surface charge for the cone channel (Haynes, 1995b), the Gouy-Chapman theory (e.g., McLaughlin, 1977) would predict a shift in the external surface potential of −15.4 mV. By itself this would reduce $K_{D(0)}$ by only 22%, which is significantly less than the 68% reduction observed ($p <$ 0.025, one-sided Student's *t*-test). Therefore, external permeant ions must compete with the blocker applied from the intracellular side, and the binding site of the blocker is indeed within the ion-conducting pore of the cone channel. The observation that tetraalkylammonium ions are impermeant in rod (Menini, 1990; Picco and Menini, 1993) and cone (Picones and Korenbrot, 1992; Fig. 1 here), together with the observation here that these blockers act within the cone channel pore, justifies the use of the Woodhull formalism in analyzing the results that follow.

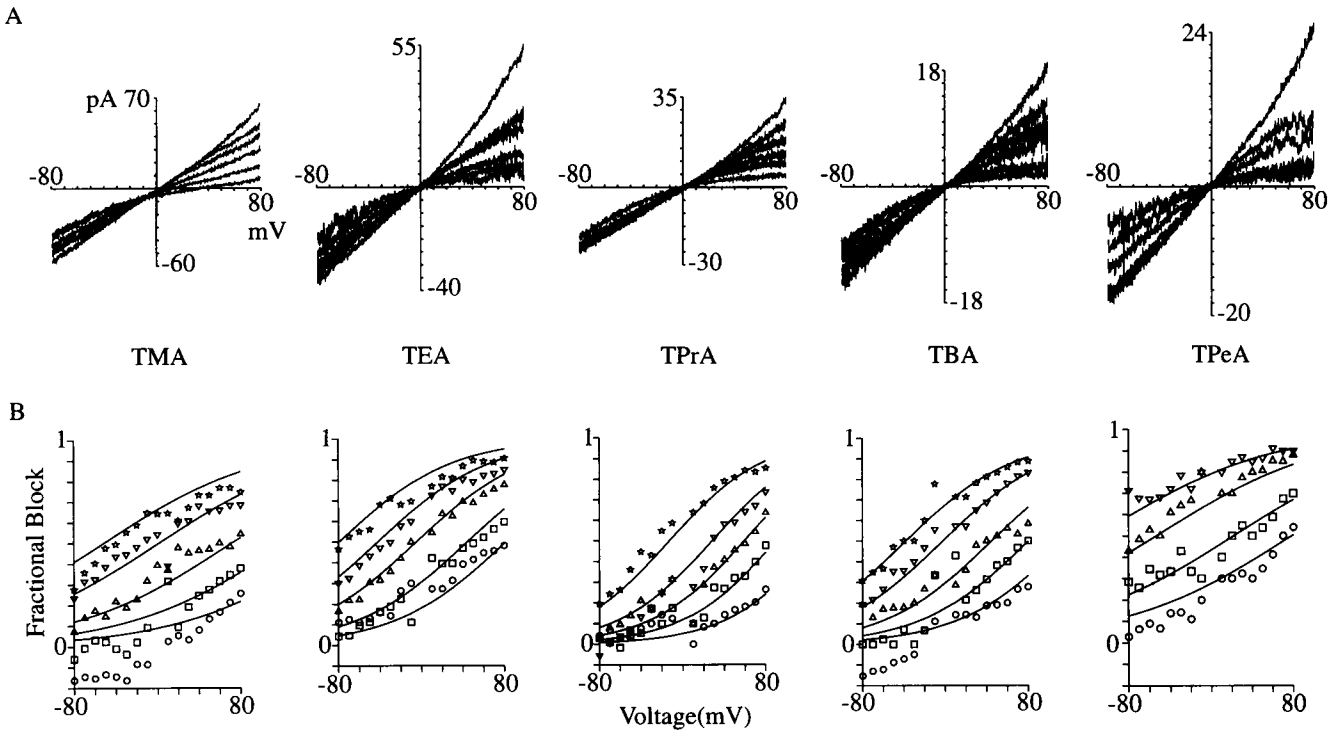

FIGURE 4 Tetraalkylammonium compounds block the rod channel from the cytoplasmic side. TMA, TEA, TPrA, TBA, or TPeA (from left to right) was substituted on an equimolar basis for sodium on the cytoplasmic side of the channel at the same concentrations given in Fig. 3 (with the exception of TPrA, which were 0, 0.2, 0.5, 1, 2, 5 mM). (*A*) Current-voltage relations. Each plot represents data obtained from a different patch. (*B*) Fractional block as a function of voltage for each of the current-voltage relations in *A*. Symbols represent the different concentrations of blocker (○, □, △, ▽, and ☆, from lowest to highest). Solid lines are fits of Eq. 2, with all points in a given plot fitted simultaneously. $K_{D(0)}$ and δ for each patch were (respectively) 50.9 mM and 0.33 for TMA, 4.7 mM and 0.44 for TEA, 3.8 mM and 0.57 for TPrA, 0.48 mM and 0.49 for TBA, and 0.054 mM and 0.20 for TPeA.

Block by tetraalkylammonium compounds from the intracellular side

Because the substituted ammonium compounds are impermeant blockers of the pore of the channel, they can be used as probes of the electrical and physical structure of the pore mouths. Tetraalkylammonium compounds with different alkyl chain lengths were used to obtain information about the physical characteristics of the blocker's binding site, and the voltage dependence of block was measured to obtain information about the position of the blocker's binding site relative to the voltage drop across the channel. A series of experiments conducted using the tetramethyl through tetrapentyl derivatives of ammonium are shown in Figs. 3 (cones) and 4 (rods). For both rod and cone channels, the block by tetraalkylammonium compounds was both concentration and voltage dependent. Furthermore, the affinity of the channel for the blocker increased with carbon chain length in both channel types.

The fraction of conductance blocked by the tetraalkylammonium compounds was calculated for each concentration and plotted as a function of voltage (Fig. 3 *B*, cones; Fig. 4 *B*, rods). As expected for a positively charged blocker entering the pore from the cytoplasmic side, the amount of block produced by each blocker increased monotonically as the potential across each membrane patch was made more positive. No relief of block was observed in any experiment, even at the most positive potentials tested (+80 mV), consistent with the action of an impermeant blocker and with the conclusion of the biionic experiments in Fig. 1.

For each experiment, all of the data points for a given patch were fitted with the Woodhull model (Eq. 2) simultaneously to yield a single estimate of each of the two fitted parameters: $K_{D(0)}$ (the dissociation constant at 0 mV) and δ (the fraction of the transmembrane voltage drop crossed by the blocker to reach its binding site). The values of these parameters for each of the tetraalkylammonium derivatives and the number of experimental trials are summarized in Table 1. As the alkyl chains were increased in length, the values obtained for $K_{D(0)}$ decreased. Comparing the mean $K_{D(0)}$ values between rod and cone channels for a given blocker showed that, on average, the values for the rod channel were 49% that of the cone channel. The fits obtained by the Woodhull model are consistent with a single molecule of blocker occupying the channel. This was confirmed by fitting the concentration dependence of block at a given voltage by the Hill equation (data not shown). In all cases, the Hill coefficient (the minimum number of binding sites) was ≤ 1, consistent with a single molecule of blocker occluding the channel.

TABLE 1 Summary of Woodhull model parameters for block of rod and cone cGMP-gated channels

	Cone			Rod		
Blocker	$K_{D(0)}$ (mM)	δ	n	$K_{D(0)}$ (mM)	δ	n
TMA_i	75 ± 35	0.38 ± 0.16*	7	44 ± 40	0.28 ± 0.11	8
TEA_i	11 ± 8	0.41 ± 0.16*	9	3.1 ± 1.5	0.32 ± 0.13	5
$TPrA_i$	4.7 ± 2.7	0.42 ± 0.14*	9	3.6 ± 1.3	0.58 ± 0.09	6
TBA_i	0.57 ± 0.11	0.48 ± 0.12*	4	0.29 ± 0.13	0.33 ± 0.17	6
$TPeA_i$	0.083 ± 0.023	0.35 ± 0.09*	5	0.024 ± 0.006	0.30 ± 0.05	4
$Tris_i$	32 ± 14	0.47 ± 0.19*	4	ND		
$NMDG_i$	85 ± 51	0.59 ± 0.26	11	ND		
TMA_o	144 ± 91	0.13 ± 0.05#	3	No block		7

The subscript i indicates that the blocker was applied from the intracellular side of the channel; o, from the extracellular side.
* Significantly different from the location of the permeant ion-binding site (0.61 from the intracellular side) at $p < 0.05$.
# Significantly different from the location of the permeant ion-binding site (0.39 from the extracellular side) at $p < 0.05$.
ND, Not determined.

Binding energy is proportional to alkyl chain length

From the amount of energy involved in the binding of the blocker to the channel, it is possible to infer the nature of the interaction between the blocker and the walls of the channel mouth: ionic bonds involve more energy than hydrogen bonds, which involve more energy than hydrophobic interactions. Given the dissociation constant, the energy of interaction between the blocker and the channel can be obtained from Eq. 3. As the carbon chain length (and hydrophobicity) increased, the energy of interaction increased monotonically for both cone (Fig. 5 *A*, $n = 34$) and rod (Fig. 5 *B*, $n = 29$) channels. The slopes of the regression lines in Fig. 5 are -3.97 kJ mol^{-1} (-950 cal mol^{-1}) for the cone channels and -4.01 kJ mol^{-1} (-958 cal mol^{-1}) for the rod channels for each carbon added (symmetrically) to the alkyl chains. Because these slopes are not significantly different, the addition of a carbon to the length of the blocker side chain contributes the same amount of energy to binding regardless of the type of channel. The amount of binding energy contributed by each carbon is consistent with hydrophobic interactions (e.g., 5 kJ mol^{-1} for van der Waals' forces) between the amino acids lining the ion channel pore and the blockers.

Position of the intracellular binding site

The mean values of δ (Table 1) for each blocker are not very different from each other, suggesting that there is a single position within the voltage drop of the cone or rod pore to which the tetraalkylammonium compounds bind. This is illustrated more clearly in Fig. 6, which shows δ from each experiment as a function of alkyl chain length. For both types of channel, the slopes of the regression line fitted to the data were statistically indistinguishable from 0. Therefore, the location of the binding site is independent of the length of the alkyl side chain. The mean value of δ from all of the tetraalkylammonium compounds is 0.41 ± 0.14 for cones ($n = 34$) and 0.36 ± 0.16 for rods ($n = 29$). These values, like the slopes, were not significantly different from each other, suggesting that the location of the intracellular tetraalkylammonium binding site is the same in both rod and cone channels. Fig. 6 also illustrates that blockers of all sizes were capable of binding to any electrical position between 0.19 and 0.65 within the cone or between 0.095 and 0.68 within the rod transmembrane voltage drop.

The Eyring rate theory model used by Haynes (1995b) to explain ion permeation through the cone channel suggests that there is a single binding site for permeant cations located 61% of the way across the voltage drop from the cytoplasmic side of the channel. For all of the tetraalkylammonium blockers tested, the binding site of the blocker was significantly different from this value ($p < 0.05$; see Table 1). Thus the tetraalkylammonium compounds do not bind to the permeant ion-binding site inferred from Eyring rate theory.

Sources of variability

It is clear from Fig. 6 and from the values presented in Table 1 that the parameters obtained by fitting the Woodhull model were quite variable. This variability in $K_{D(0)}$ and δ could be the result of one of four processes. First, it could be the result of experimental error. If, for example, block were not reversible or if the current were reduced by a leak subtraction error or by loss of channels, then the estimates of $K_{D(0)}$ and δ would be biased. Care was taken throughout these experiments to ensure that the leak currents before and after blocker application were the same and that the currents in the absence of blocker at the beginning and the end of the experiment were the same. Second, variability could be an artifact of the fitting process, either because of an error in the fitting procedure or because $K_{D(0)}$ and δ are not completely independent of each other in the fitting procedure. The latter possibility seems unlikely because the parameter cross-correlation matrix generated by our curve-fitting routine (a Levenberg-Marquardt routine; Press et al., 1992) shows that $K_{D(0)}$ and δ are negatively correlated; yet we find the parameters themselves are positively correlated. That is, the deeper the blocker goes, the higher the value of $K_{D(0)}$

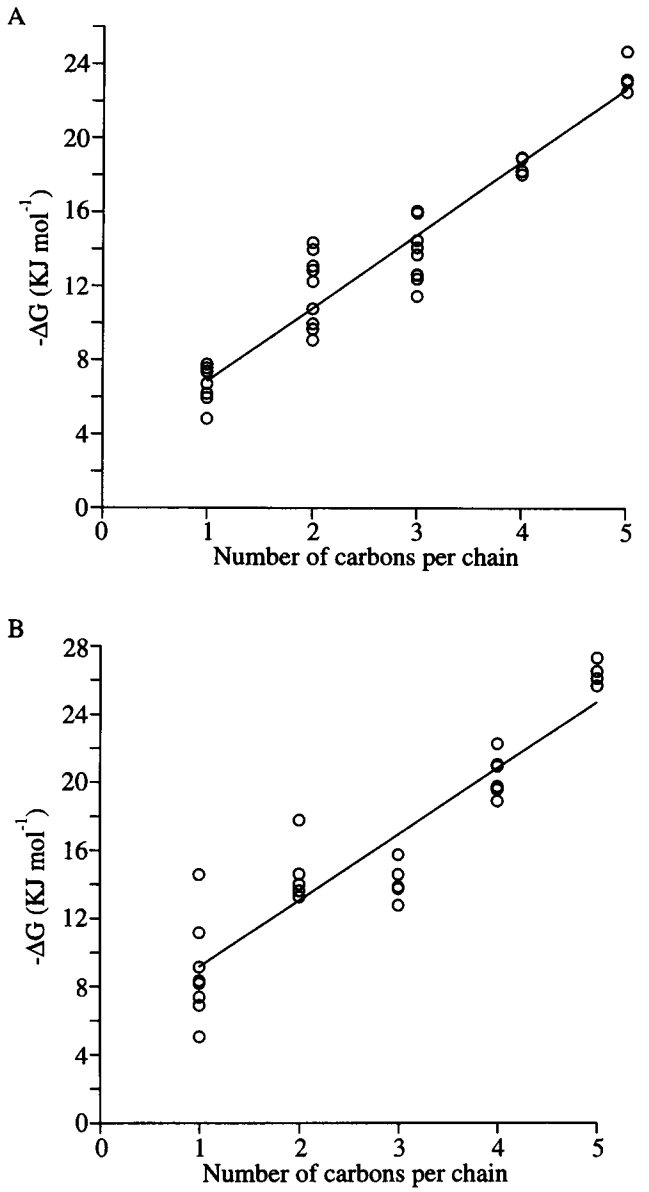

FIGURE 5 Binding energy is directly proportional to alkyl chain length. Binding energy was calculated using Eq. 3 and dissociation constants from experiments like those in Figs. 3 and 4. Each point represents a different experiment. Lines are linear regressions. (*A*) Cone channels. The regression line had a slope of -3.97 kJ mol^{-1} per carbon, a *y* intercept of -2.88 kJ mol^{-1}, and a correlation coefficient of 0.95. (*B*) Rod channels. The regression line had a slope of -4.01 kJ mol^{-1} per carbon, a *y* intercept of -4.71 kJ mol^{-1}, and a correlation coefficient of 0.92.

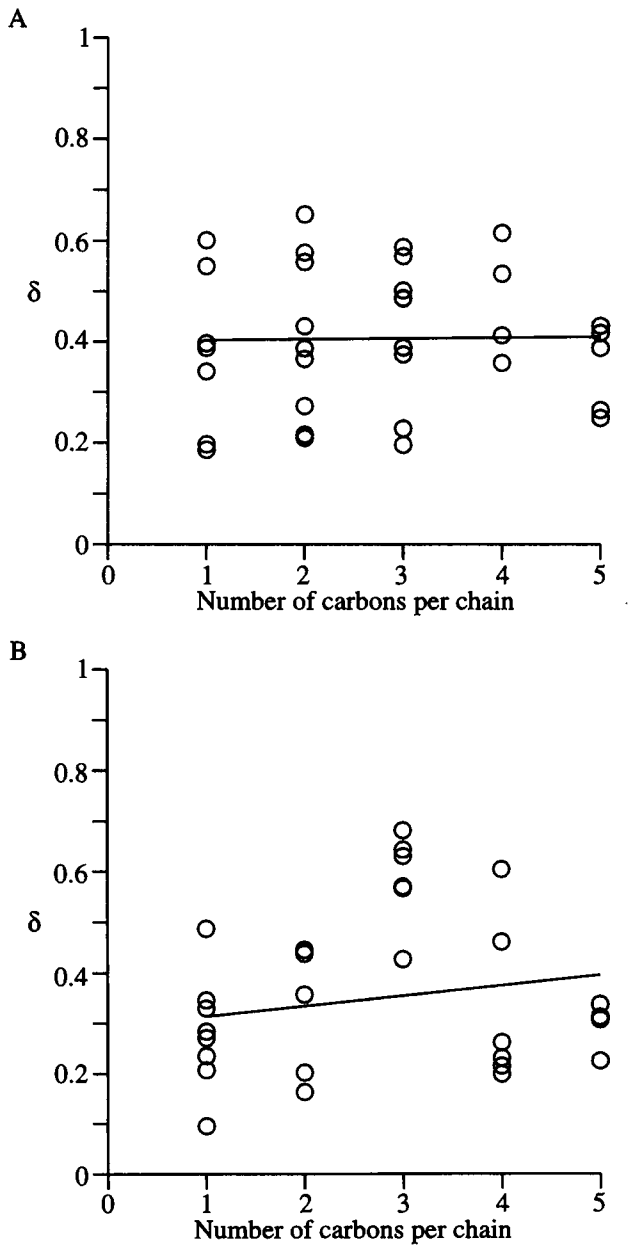

FIGURE 6 Location of the blocker binding site is independent of alkyl chain length. δ values were determined for each patch exposed to blocker. Each symbol represents a different experiment. Lines are linear regressions. (*A*) Cone channels. The linear regression line had a slope of 0.0016 per carbon, a *y* intercept of 0.402, and a correlation coefficient of 0.0156. (*B*) Rod channels. The linear regression had a slope of 0.014 per carbon, a *y* intercept of 0.33, and a correlation coefficient of 0.122. The slopes of the regression lines in *A* and *B* were not different from 0, nor were the slopes or intercepts different from each other.

(data not shown). We checked the consistency of the fitting procedure by fitting the data twice. In the first case, we fitted voltage dependence of block at all concentrations of blocker. In the second case, we fitted the concentration dependence of block at all voltages. The values obtained for $K_{D(0)}$ and δ were the same for both procedures. A third possibility is that not all of the patches are identical, and so variability arises between patches. Fourth, variability could arise from within a given patch. To distinguish between the last two possibilities, the parameters of the Woodhull model were estimated by separately fitting the voltage dependence of block at each concentration in a patch, rather than fitting all concentrations simultaneously. The mean values for the parameters obtained by this method were not significantly different from those obtained by fitting the data simultaneously. Thus all of the variability can be accounted for by the variability within a given patch, indicating that the

observed variability is intrinsic to the channels in a given patch rather than between patches or as a result of the fitting process. If variability arises within a given patch, then repeated applications of the same blocker should give different results. Table 2 summarizes the values of $K_{D(0)}$ and δ obtained from a cone patch during repeated application of 20 mM TEA over a period of 23 min. These results indicate that the process inducing this variability occurs within a patch on a relatively slow time scale (seconds to minutes). Because there is no systematic change over time, the process must be reversible in the absence of ATP or energy sources other than the electrochemical gradient.

If this variability is real, then the variability of the location of the blocker binding sites may be interpreted in two ways. In the first case, there might be a series of binding sites that could be occupied. This seems unlikely, because a sufficiently high voltage should force the blocker to the limiting location, and this is not observed. In the second case, there might be a single, discrete binding site, but flexibility in the channel's structure alters the electric field that the blocker experiences.

Size of the intracellular mouth of the channel

As shown in Figs. 3 and 4, tetraalkylammonium compounds up to the size of TPeA were able to block both the rod and cone channel in a voltage-dependent manner. However, THxA blocked both the cone (Fig. 7 *A*) and rod (Fig. 7 *B*) channel in a voltage-independent manner. This suggests that THxA is interacting with the channel outside of the transmembrane voltage drop and is not capable of entering the channel. Therefore, the diameter of the cone and rod inner channel mouth must be larger that TPeA, but smaller than THxA. It is difficult to be more precise about the diameter of the mouth, both because the alkyl chains of these tetraalkylammonium derivatives are quite flexible (with free rotation occurring around their carbon-carbon bonds) and because the extent of interdigitation (if any) of the alkyl chains into the walls of the pore is unknown. Assuming no interdigitation and the smallest conformation of TPeA, the lower bound for the estimated diameter of the intracellular mouth of the pore is ~12 Å.

Block by Tris and *N*-methyl-D-glucamine from the intracellular side

The increment in binding energy associated with adding one carbon to each of the four alkyl chains of a tetra-

TABLE 2 Repeated exposure of cone cGMP-gated channels to 20 mM TEA shows that Woodhull model parameters are variable

Time (min)	$K_{D(0)}$	δ
3	20.46	0.565
10	22.62	0.597
16	18.62	0.677
23	15.38	0.524

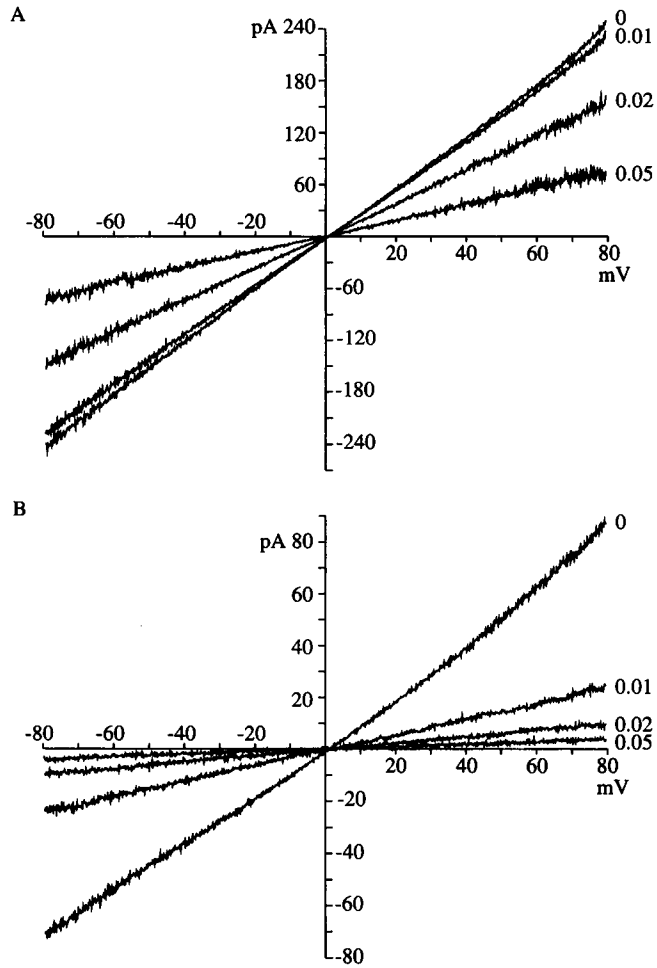

FIGURE 7 THxA blocks both cone and rod cGMP-gated channels in a voltage-independent manner. Current-voltage relations were formed for cone (*A*) and rod (*B*) patches exposed to THxA on the cytoplasmic side of the channel. The concentrations of THxA (in mM) are given at the right of the traces.

alkylammonium compound suggests that these blockers interact with the walls of the channel pore via hydrophobic interactions. Hydrogen bonds would also stabilize blocker interaction, but such bonds are not possible with these tetraalkylammonium compounds. Two commonly used cations, Tris and NMDG, were used to determine whether the pore also contains groups that can form hydrogen bonds. Both Tris and NMDG contain several hydroxyl groups that could form hydrogen bonds. Tris is similar in size to TEA, and contains three hydroxyl groups. The larger NMDG is essentially a methylammonium head followed by a six-carbon hydrophilic tail containing five hydroxyl groups. If hydrogen bonding is possible, then these compounds should be better blockers than similarly sized tetraalkylammonium blockers.

Both Tris and NMDG block the cone channels in a voltage- and concentration-dependent fashion (Fig. 8). The values for $K_{D(0)}$ and δ obtained by fitting the fractional block with the Woodhull model (Eq. 2) are given in Table

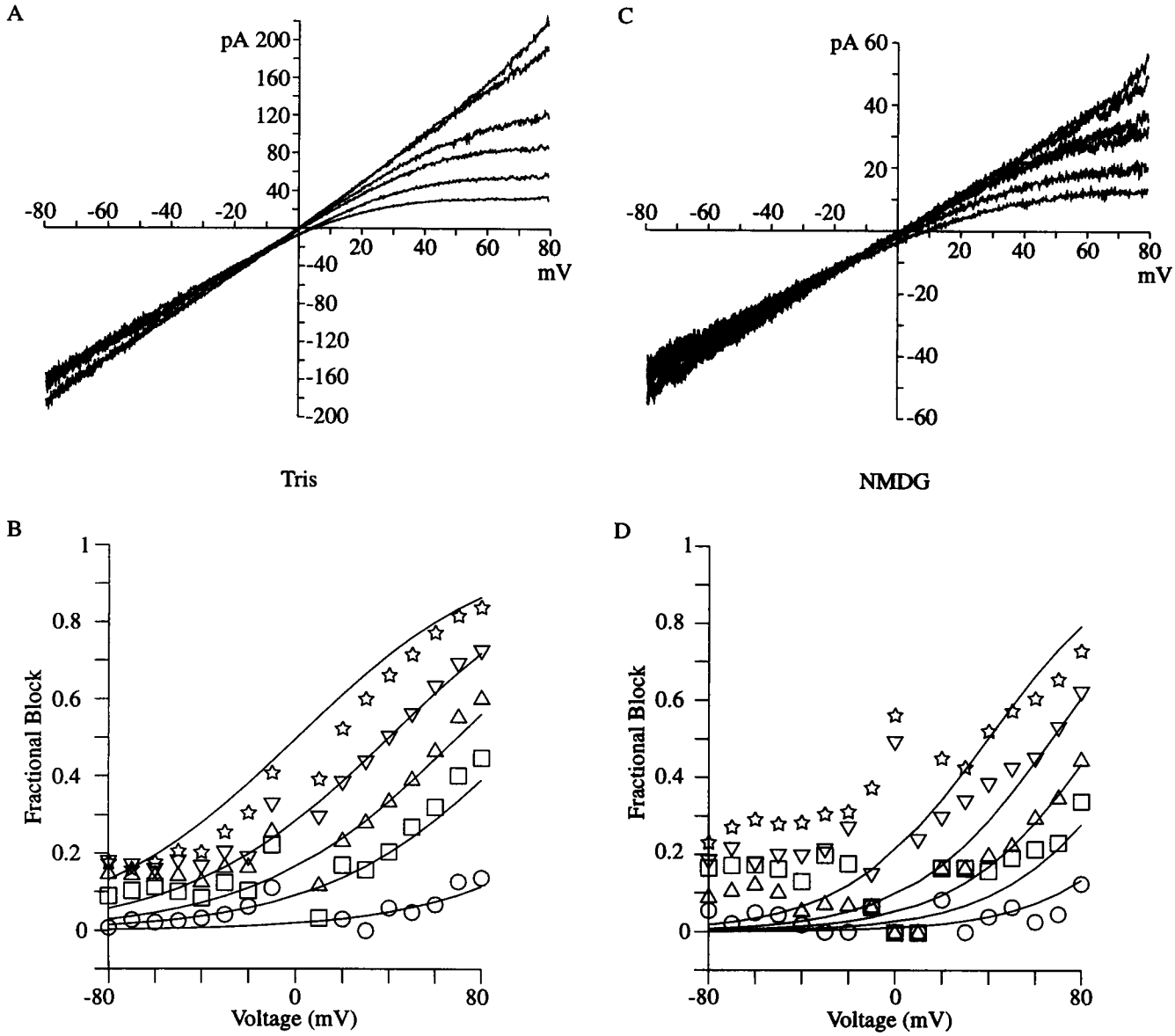

FIGURE 8 Block of the cone channel by hydroxyl-containing ammonium derivatives. Both Tris and NMDG contain hydroxyl groups that are available for hydrogen bond formation. Tris or NMDG was substituted on an equimolar basis for sodium on the cytoplasmic side of the channel. Tris was applied in concentrations of 0, 1, 5, 10, 20, and 50 mM; NMDG, 0, 2, 5, 10, 20, and 50 mM. Current-voltage relations are shown for Tris (*A*) and NMDG (*C*). Different patches are shown in *A* and *C*. The shift in reversal potential can be accounted for by the shift in the Nernst potential for sodium. (*B, D*) Fractional block as a function of voltage from current-voltage relations in *A* and *C*. Symbols represent different concentrations of blocker (○, □, △, ▽, and ☆, from lowest to highest). Solid lines are fits of Eq. 2 to the data at positive potentials only. $K_{D(0)}$ and δ for each patch were (respectively) 41 mM and 0.59 for Tris, and 188 mM and 0.84 for NMDG. No compensation was made for the extent of Tris ionization (~80% of concentration as mixed).

1. A comparison of the mean δ values obtained for NMDG and Tris with those obtained for the tetraalkylammonium compounds indicate that Tris binds at a position no different from the average tetraalkylammonium binding site, whereas NMDG binds to a position farther into the transmembrane voltage drop. In fact, the mean position of NMDG binding is not significantly different from the cone channel's permeant ion-binding site (δ = 0.61; Haynes, 1995b). The ability of NMDG to enter so deeply into the channel pore is likely due to the closer similarity of its head (methylammonium) to ammonium, which is capable of permeating the cone channel (Haynes, 1995a). Thus the methylammonium headgroup may allow the compound access to the permeant ion-binding site, whereas the addition of a long hydrophilic tail may act as an anchor, preventing NMDG from passing through the channel.

Comparing the mean $K_{D(0)}$ values obtained for Tris (32 ± 14) with those for TEA (11 ± 8) suggests that a decrease in blocker hydrophobicity destabilizes interactions between the blocker and cone channel pore. Although these blockers are of similar size and bind to similar locations within the transmembrane voltage drop, the values for $K_{D(0)}$ required

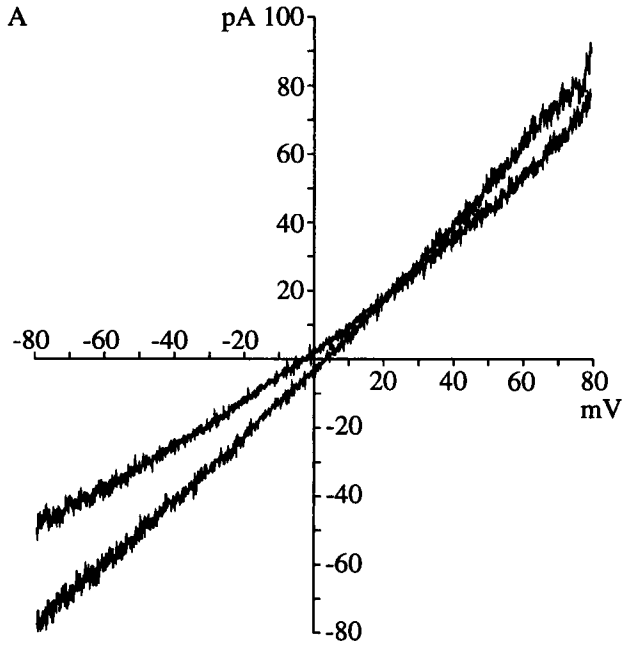

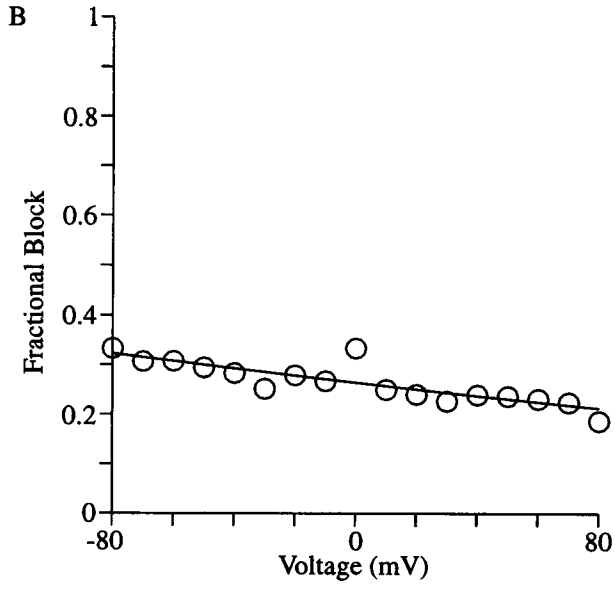

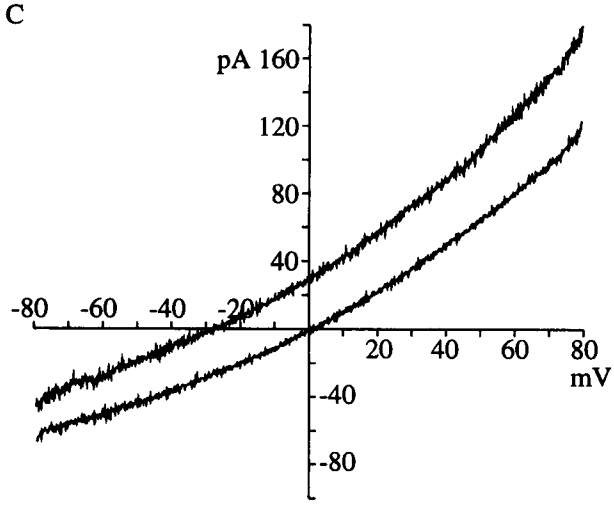

to describe Tris block are three times larger than those for TEA block. These data and those presented above suggest that the amino acids comprising the blocker binding site are purely hydrophobic in nature and cannot support the formation of hydrogen bonds.

Occasionally, as in Fig. 8 *C*, voltage-independent block by NMDG was also observed. This was not consistently observed and so was not investigated further. Its occurrence suggests that block by NMDG may be more complicated than supposed by the simple Woodhull interpretation, but the processes involved remain to be determined.

Block by extracellular TMA

Because tetraalkylammonium compounds applied from the cytoplasmic side block rod and cone channels, it was of interest to determine whether these compounds could block the channel when applied externally. TMA was applied to the extracellular side of rod or cone patches by perfusing the pipette with a 100 mM TMA solution. TMA was chosen because the shift in the reversal potential as TMA substituted for sodium would allow the concentration of TMA in the pipette to be estimated. Relatively modest concentrations of TMA (~35 mM) blocked cone channels (Fig. 9 *A*, $n = 3$), but even large concentrations (up to 90 mM) failed to block rod channels in seven of seven rod patches (Fig. 9 *C*). This suggests that the outer mouth of the rod channel lacks a tetraalkylammonium binding site and must therefore have a structure significantly different from that of the cone channel.

The values for $K_{D(0)}$ and δ obtained by fitting the fractional block of the cone conductance are given in Table 1. The values for $K_{D(0)}$ obtained for internal and external TMA block were not significantly different, suggesting that the two sites may have similar physical characteristics. On average, external TMA crossed only 13% of the voltage drop. The position of the external TMA binding site was significantly different ($p < 0.05$) from both the location of the cone channel's permeant ion-binding site (39% of the voltage drop from the outside; Haynes, 1995b) and the location of the intracellular tetraalkylammonium site. These data suggest that there are two TMA-binding sites that lie at opposite ends of the cone cGMP-gated channel pore. Because TMA presented to the cytoplasmic surface of the patch was incapable of accessing the external binding site (and vice versa), the two sites must be physically separated from each other. The location of the region between the two tetraalkylammonium-binding sites is consistent with the

FIGURE 9 Block by external TMA. (*A*) Current-voltage relation from a cone patch. TMA (100 mM) was perfused into the pipette. The reversal potential was used to estimate the concentration of blocker bathing the extracellular surface of the membrane patch (35 mM in this case). (*B*) Voltage dependence of fractional block. The fraction of conductance blocker by the organic cation was plotted as a function of voltage and fit with Eq. 2. $K_{D(0)} = 100$ mM and $\delta = 0.082$. (*C*) External TMA did not block rod channels. The estimated TMA concentration was 92 mM.

proposed location of the permeant ion-binding site (Haynes, 1995b).

DISCUSSION

The results described here confirm previous reports that rod (Menini, 1990; Picco and Menini, 1993) and cone (Picones and Korenbrot, 1992) cGMP-gated channels are unable to conduct tetraalkylammonium compounds. Our results characterize the block of sodium conduction produced by these compounds in both rod and cone cGMP-gated channels. The voltage dependence of block suggests that the tetraalkylammonium compounds cross a portion of the transmembrane voltage drop within the channel pore. That the location of the intracellular binding site was within the pore was confirmed by evidence of competition by extracellular permeant ions, because the affinity of the blocker for its intracellular binding site increased when competition by extracellular sodium was reduced.

In both rod and cone channels, the data suggest that there is a single interior binding site for tetraalkylammonium compounds. This site is located ~40% of the way across the transmembrane voltage drop from the intracellular side. The properties of this site (hydrophobic) suggest that it is distinct from the permeant ion-binding site (a high field strength site; Picones and Korenbrot, 1992; Haynes, 1995a,b). The variability in δ values suggests that there may be flexibility in the channel structure or some form of rapid and reversible modulation with associated changes in the voltage field. The monotonic decrease in $K_{D(0)}$ with increasing alkyl chain length and the binding energy increment for each carbon added suggest that the binding site is hydrophobic, and the increase in $K_{D(0)}$ with the addition of hydroxyl groups suggests that the residues that make up the site do not form hydrogen bonds with the blockers. The diameter of the intracellular mouth of the pore must be larger than TPeA but smaller then THxA. Overall, the properties of the intracellular tetraalkylammonium-binding site are similar in rod and cone channels. The only major difference between the intracellular sites of the two channels is that the dissociation constant at 0 mV of the rod channel is ~51% lower than for the cone channel.

The cone, but not the rod, channel contains a second tetraalkylammonium-binding site that is accessible only from the external surface. This site is located ~13% of the way across the voltage drop from the extracellular side and is distinct from the proposed location of the permeant ion-binding site (~39%; Haynes, 1995b). Although experimental limitations prevented complete characterization of this site, a comparison of internal and external binding affinities suggests that the internal and external sites may have similar properties. The lack of an external tetraalkylammonium-binding site in the rod channel indicates that the rod and cone channel subtypes have significant structural differences in the outer mouth region.

The properties of the two tetraalkylammonium binding sites are inconsistent with those expected for the strong-field permeant ion-binding site described by permeation studies (Picones and Korenbrot, 1992; Haynes, 1995a,b) and suggest that the permeant ion-binding site lies more centrally in the pore than the tetraalkylammonium-binding sites. The location of the permeant ion-binding site inferred by placement of the tetraalkylammonium-binding sites and by the location of the NMDG-binding site is remarkably consistent with that proposed by Haynes (1995b) on the basis of Eyring rate theory modeling of ion permeation. The positions of the tetraalkylammonium sites are roughly consistent with the locations of the barriers to permeant ion entry suggested by the Eyring model. The data presented here also suggest that the extracellular mouth of the channel is shallower than the intracellular mouth of the channel, and that the permeant ion-binding site is located in the narrowest portion of the pore. Permeability studies show that the cone cGMP-gated channel is capable of conducting alkali metal cations up to the size of cesium (Picones and Korenbrot, 1992; Haynes, 1995a), suggesting that the narrowest part of the cone channel has a diameter of at least 3.4 Å. The ability of NMDG to reach the permeant ion-binding site suggests that the narrowest part of the pore is somewhat larger than this, at least the size of methylammonium.

Similarities in the pores of ligand- and voltage-gated channels

By characterizing the pore of the cGMP-gated channels with organic blockers, we have confirmed that similarities exist between the pore regions of these ligand-gated channels and those of the voltage-gated potassium channel family. Channels from both families contain a single tetraalkylammonium-binding site within their inner vestibules. In potassium channels this site is also hydrophobic in nature (French and Shoukimas, 1981; Coronado and Miller, 1982; see Yellen, 1987, for a review). The relative sizes of inner vestibules are also similar, each being capable of holding the large TPeA blocker (French and Shoukimas, 1981). Not all subtypes of the potassium channel family contain an external tetraalkylammonium compound binding site, and those that do selectively bind TEA (Villaroel et al., 1988). Within the cGMP-gated channel family, only the cone subtype contains an external tetraalkylammonium-binding site. This site bound TMA, but the selectivity of the site for other tetraalkylammonium compounds is unknown. Based on the data presented here, the structural similarities between the cGMP-gated nonspecific cation channels and voltage-gated potassium channels seen in cDNA sequence analysis (Jan and Jan, 1990; Kaupp, 1991; Bönigk et al., 1993) are reflected in the biophysical properties of the channels.

We wish to thank Drs. R. J. French, K. Sharkey, and K. Hoehn for helpful discussion of these experiments.

REFERENCES

Bodoia, R. D., and P. B. Detwiler. 1985. Patch-clamp recordings of the light-sensitive dark noise in retinal rods from the lizard and frog. *J. Physiol. (Lond.).* 367:183–216.

Bönigk, W., W. Altenhofen, F. Muller, A. Dose, M. Illing, R. S. Molday, and U. B. Kaupp. 1993. Rod and cone photoreceptor cells express distinct genes for cyclic GMP-gated channels. *Neuron.* 10:865–877.

Colamartino, G., A. Menini, and V. Torre. 1991. Blockage and permeation of divalent cations through the cyclic GMP-activated channel from tiger salamander rods. *J. Physiol. (Lond.).* 440:189–206.

Coronado, R., and C. Miller. 1982. Conduction and block by organic cations in a K^+-selective channel from sarcoplasmic reticulum incorporated into planar phospholipid bilayers. *J. Gen. Physiol.* 79:529–547.

Dhallan, R. S., K.-W. Yau, K. A. Schrader, and R. R. Reed. 1990. Primary structure and functional expression of a cyclic nucleotide-activated channel from olfactory neurons. *Nature.* 347:184–187.

French, R. J., and J. J. Shoukimas. 1981. Blockade of squid axon potassium conductance by internal tetra-*n*-alkylammonium ions of various sizes. *Biophys. J.* 34:271–291.

Furman, R. E., and J. C. Tanaka. 1990. Monovalent selectivity of the cyclic guanosine monophosphate-activated ion channel. *J. Gen. Physiol.* 96: 57–82.

Gray, P., and D. Attwell. 1985. Kinetics of light-sensitive channels in vertebrate photoreceptors. *Proc. R. Soc. Lond.* B223:379–388.

Haynes, L. W. 1992. Block of the cyclic GMP-gated channel of vertebrate rod and cone photoreceptors by L-*cis*-diltiazem. *J. Gen. Physiol.* 100: 783–801.

Haynes, L. W. 1993. Mono- and divalent cation selectivity of catfish cone cGMP-gated channels. *Biophys. J.* 66:A133.

Haynes, L. W. 1995a. Permeation of internal and external monovalent cations through the catfish cone photoreceptor cGMP-gated channel. *J. Gen. Physiol.* 106:485–505.

Haynes, L. W. 1995b. Permeation and block by internal and external divalent cations of the catfish cone photoreceptor cGMP-gated channel. *J. Gen. Physiol.* 106:507–523.

Haynes, L. W., A. R. Kay, and K.-W. Yau. 1986. Single cyclic GMP-activated channel activity in excised patches of rod outer membrane. *Nature.* 321:66–70.

Haynes, L. W., and S. C. Stotz. 1996. Modulation of rod, but not cone, cGMP-gated photoreceptor channels by calcium-calmodulin. *Visual Neurosci.* In press.

Haynes, L. W., and K.-W. Yau. 1990. Single-channel measurements from the cyclic GMP-activated conductance of catfish retinal cones. *J. Physiol. (Lond.).* 249:451–481.

Jan, L. Y., and Y. N. Jan. 1990. A superfamily of ion channels. *Nature.* 345:672.

Karpen, J. W., A. L. Zimmerman, L. Stryer, and D. A. Baylor. 1988a. Gating kinetics of the cyclic GMP-activated channel of retinal rods: flash photolysis and voltage-jump studies. *Proc. Natl. Acad. Sci. USA.* 85:1287–1294.

Karpen, J. W., A. L. Zimmerman, L. Stryer, and D. A. Baylor. 1988b. Molecular mechanics of the cyclic GMP-activated channel of retinal rods. *Cold Spring Harb. Symp. Quant. Biol.* 53:325–332.

Kaupp, U. B., T. Niidome, T. Tanabe, S. Terada, W. B'nigk, W. Sthhmer, N. J. Cook, K. Kangawa, H. Matsuo, T. Hirose, T. Miyata, and S. Numa. 1989. Primary structure and functional expression from complementary DNA of the rod photoreceptor cyclic GMP-gated channel. *Nature.* 342:762–766.

Kaupp, U. B. 1991. The cyclic nucleotide-gated channels of vertebrate photoreceptors and olfactory epithelium. *Trends Neurosci.* 14:150–156.

Lagnado, L., and D. A. Baylor. 1992. Signal flow in visual transduction. *Neuron.* 8:995–1002.

Ludwig, J., T. Margalit, E. Eismann, D. Lancet, and U. B. Kaupp. 1990. Primary structure of cAMP-gated channel from bovine olfactory epithelium. *FEBS Lett.* 270:24–29.

McLaughlin, S. 1977. Electrostatic potentials at membrane-solution interfaces. *Curr. Top. Membr. Transp.* 9:71–144.

Menini, A. 1990. Currents carried by monovalent cations through cGMP-activated channels in excised patches from salamander rods. *J. Physiol. (Lond.).* 424:167–185.

Perry, R. J., and P. A. McNaughton. 1991. Response properties of cones from the tiger salamander. *J. Physiol. (Lond.).* 433:561–587.

Picco, C., and A. Menini. 1993. The permeability of the cGMP-activated channel to organic cations in retinal rods of the tiger salamander. *J. Physiol. (Lond.).* 460:741–758.

Picones, A., and J. I. Korenbrot. 1992. Permeation and interaction of monovalent cations with the cGMP-gated channel of cone photoreceptors. *J. Gen. Physiol.* 100:647–673.

Press, W. H., S. A. Teukolsky, W. T. Vetterling, and B. P. Flannery. 1992. Numerical Recipes in C: The Art of Scientific Computing, 2nd ed. Cambridge University Press, Cambridge, England. 994.

Stotz, S. C., and L. W. Haynes. 1995. Block of cone cGMP-gated channels by internal organic cations. *Biophys. J.* 68:A386.

Stryer, L. 1986. Cyclic GMP cascade of vision. *Annu. Rev. Neurosci.* 9:87–119.

Taylor, W. R., and D. A. Baylor. 1995. Conductance and kinetics of single cGMP-activated channels in salamander rod outer segments. *J. Physiol. (Lond.).* 483:567–582.

Villaroel, A., O. Alvarez, A. Oberhauser, and R. Latorre. 1988. Probing a Ca^{2+}-activated K^+ channel with quaternary ammonium ions. *Pflugers Arch.* 413:118–126.

Woodhull, A. M. 1973. Ionic blockade of sodium channels in nerve. *J. Gen. Physiol.* 61:687–708.

Yau, K.-W., and L. W. Haynes. 1986. Effect of divalent cations on the macroscopic cGMP-activated current in excised rod membrane patches. *Biophys. J.* 49:33a.

Yellen, G. 1987. Permeation in K^+ channels: implications for channel structure. *Annu. Rev. Biophys. Biophys. Chem.* 16:227–246.

Zar, J. H. 1984. Biostatistical Analysis, 2nd ed. Prentice-Hall, Englewood Cliffs, NJ.

Zimmerman, A. L., and D. A. Baylor. 1986. Cyclic-GMP sensitive conductance of retinal rods consists of aqueous pores. *Nature.* 321:70–72.

Zimmerman, A. L., and D. A. Baylor. 1992. Cation interactions within the cyclic GMP-activated channel of retinal rods from the tiger salamander. *J. Physiol. (Lond.).* 449:759–783.